current, is in the opposite sense to the observed rectification. (v) The geometrical asymmetry of the curved tip and the flat sample, which can give rise to asymmetry (*2*), predicts the wrong polarity for the rectification. Compared to all the mechanisms we have examined, the DOS model is the most compatible with all the experimental observations. To more fully verify the DOS model requires a theory along the lines of the effect of single atoms on the bias dependence of the STM current (*22*) to sort out the structural from the DOS contributions.

This demonstration that molecules consisting of tens of atoms can produce asymmetry, and that a substitution can be made to allow bonding to a desired substrate, opens up a range of chemical structures that may be studied. We believe that, if the energy levels of the molecules are suitably matched to that of the electrodes, it will change the *I-V* characteristics of the STM in dramatic ways. The bonding technique may be extended so that different kinds of molecules are attached to different electrodes on the same sample (*23*). The STM may thus prove useful in measuring the electronic energy levels of adsorbed molecules, and the molecules may provide control of the STM characteristics.

REFERENCES AND NOTES

1. R. M. Tromp, R. J. Hamers, J. E. Demuth, *Science* **234**, 304 (1986).
2. R. M. Feenstra, J. A. Stroscio, A. P. Fein, *Surf. Sci.* **181**, 295 (1987).
3. W. J. Kaiser and R. C. Jaklevic, *IBM J. Res. Dev.* **30**, 411 (1986).
4. Ph. Avouris, *J. Phys. Chem.* **94**, 2246 (1990).
5. L. L. Soethout, H. Van Kempen, G. F. A. Van De Walle, *Adv. Electron. Electron Phys.* **79**, 153 (1990).
6. X. L. Wu and C. M. Lieber, *Prog. Inorg. Chem.* **39**, 431 (1991).
7. A. Aviram and M. A. Ratner, *Chem. Phys. Lett.* **29**, 277 (1974).
8. J. K. Gimzewski, E. Stoll, R. R. Schlittler, *Surf. Sci.* **181**, 267 (1987).
9. P. H. Lippel, R. J. Wilson, M. D. Miller, Ch. Wöll, S. Chiang, *Phys. Rev. Lett.* **62**, 171 (1989).
10. W. Mizutani *et al.*, *Jpn. J. Appl. Phys.* **28**, L1460 (1989).
11. W. M. Heckl *et al.*, *Langmuir* **5**, 1433 (1989).
12. A. Aviram, L. Li, M. Pomerantz, P. Roland, A. G. Schrott, in preparation.
13. W. R. Barger, A. W. Snow, H. Wohltjen, N. L. Jarvis, *Thin Solid Films* **133**, 197 (1985).
14. B. Simic-Glavaski, S. Zecevic, E. Yeager, *J. Am. Chem. Soc.* **107**, 5625 (1985).
15. P. H. Schroer and J. Becker, *IBM J. Res. Dev.* **30**, 543 (1986).
16. R. M. Tromp, *J. Phys. Condens. Matter* **1**, 10211 (1989).
17. G. Binnig *et al.*, *Europhys. Lett.* **1**, 31 (1986).
18. J. G. Simmons, *J. Appl. Phys.* **34**, 2581 (1963).
19. G. A. Haas and R. E. Thomas, in *Techniques of Metals Research*, E. Passaglia, Ed. (Interscience, New York, 1972), vol. 6, p. 91.
20. R. O. Loutfy, J. H. Sharp, C. K. Hsiao, R. Ho, *J. Appl. Phys.* **52**, 5218 (1981).
21. D. Wöhrle and D. Meissner, *Adv. Mater.* **3**, 129 (1991).
22. N. D. Lang, *Phys. Rev. B* **34**, 5947 (1986).
23. P. E. Laibinis *et al.*, *Science* **245**, 845 (1989).
24. We thank R. Kaufman and C. Joachim for the Nanoscope modifications; P. A. Roland and R. G. Schad for Auger measurements; D. W. Abraham for the loan of a Nanoscope base; A. C. Callegari, J. E. Demuth, and D. P. E. Smith for helpful discussions; and C. Pickover for the graphics of Fig. 3.

26 October 1991; accepted 2 January 1992

Rhenium-Osmium Isotope Constraints on the Age of Iron Meteorites

M. F. HORAN, J. W. MORGAN, R. J. WALKER, J. N. GROSSMAN

Rhenium and osmium concentrations and the osmium isotopic compositions of iron meteorites were determined by negative thermal ionization mass spectrometry. Data for the IIA iron meteorites define an isochron with an uncertainty of approximately ±31 million years for meteorites ~4500 million years old. Although an absolute rhenium-osmium closure age for this iron group cannot be as precisely constrained because of uncertainty in the decay constant of ^{187}Re, an age of 4460 million years ago is the minimum permitted by combined uncertainties. These age constraints imply that the parent body of the IIAB magmatic irons melted and subsequently cooled within 100 million years after the formation of the oldest portions of chondrites. Other iron meteorites plot above the IIA isochron, indicating that the planetary bodies represented by these iron groups may have cooled significantly later than the parent body of the IIA irons.

IRON METEORITES ARE DIVIDED INTO groups on the basis of their internal structures and chemical compositions. In most instances, irons of the same group were likely derived from the same parent body. Most iron meteorites, such as those in groups IIAB and IIIAB, are fragments of the cores of small planets. They are called magmatic irons because their compositions are consistent with fractional crystallization of the core of an initially chondritic body that melted to form a separate metal sulfide core and silicate mantle (*1*). Some iron meteorites, such as group IAB irons, are termed nonmagmatic irons because their chemical compositions suggest that they originated as silicate-metal segregations resulting from impact on or near the surface of their parent body. Determining the crystallization ages of iron meteorite groups to within several tens of millions of years is critical to understanding the timing of parent body accretion, melting, segregation of metal, and subsequent cooling. However, the ages of iron meteorite groups are still poorly constrained. Conventional long-lived radiogenic isotopes such as U, Th, K, Sm, Rb, and Lu are not useful for directly dating irons because of their low abundances in metallic phases. These isotopic systems have generally been applied only to dating silicate inclusions within some iron groups (*2–6*). Studies of the Pd-Ag system, based on the decay of ^{107}Pd to ^{107}Ag (half-life of 6.5 × 10^6 years) (*7–10*), apparently limits the age of IIB and IIIAB meteorites to no more than about 65 million years (10 half-lives) younger than the maximum age [~4560 million years ago (Ma)] of calcium-aluminum inclusions in chondrites (*11*). Absolute Pd-Ag ages cannot be determined, however, because the initial ^{107}Pd/^{108}Pd ratio is not known.

The highly siderophile elements Re and Os occur in relatively high abundances in many iron meteorites. The Re-Os isotope system (^{187}Re→^{187}Os by β decay) is thus ideal for dating iron meteorite groups. Early attempts to apply the system to dating irons, however, suffered from the poor precision of the analytical techniques (*12*). The subsequent application of ion microprobe and resonance ionization mass spectrometry techniques significantly improved precision. Luck and co-workers (*13, 14*) analyzed iron meteorites from different groups (IA, IIA, IIIA, and IVAB) and obtained a Re-Os isotope isochron with a slope of 0.0706 ± 0.0014; Walker and Morgan (*15*) obtained results for two irons (IA and IIA) that were consistent with this isochron. Luck and Allègre (*14*) also combined their iron data with results for metal separated from ordinary chondrites and obtained an isochron with a slope of 0.0716 ± 0.0019. They assumed that the age of iron meteorites and ordinary chondrites is 4550 Ma and used the isochron to determine a decay constant of 1.52 ± 0.04 × 10^{-11} year^{-1}. A significantly different decay con-

---

M. F. Horan and J. W. Morgan, U.S. Geological Survey, Mailstop 981, Reston, VA 22092.
R. J. Walker, Isotope Geochemistry Laboratory, Department of Geology, University of Maryland, College Park, MD 20742.
J. N. Grossman, U.S. Geological Survey, Mailstop 990, Reston, VA 22092.

Table 1. Abundances of Re and Os and Os isotopic ratios in IA, IIA, IIB, and IIIA iron meteorites. Concentrations are in parts per billion; 2σ uncertainities for Re and Os concentrations are approximately ±0.2% (except for Mount Joy for which the Re uncertainty is ±0.4%); 2σ uncertainties for ratios are 1 per mil for the ^{187}Os/^{186}Os ratios and 3 per mil for ^{187}Re/^{186}Os ratios (except for Mount Joy, which is 5 per mil).

Meteorite	Type	Re	Os	^{187}Re/^{186}Os	^{187}Os/^{186}Os
Canyon Diablo	IA	198.9	2,047	3.906	1.1117
Negrillos	IIA	4,816	65,740	2.941	1.0300
Bennett County	IIA	4,501	58,260	3.102	1.0441
Coahuila	IIA	1,241	10,310	4.844	1.1788
Coahuila (dup.)	IIA	1,240	10,310	4.840	1.1805
N. Chile (Tocopilla)	IIA	203.2	1,057	7.763	1.4074
N. Chile (Filomena)	IIA	203.4	1,068	7.688	1.4004
Lombard	IIA	158.7	797.2	8.042	1.4320
Mount Joy	IIB	23.00	143.1	6.483	1.3209
Costilla Peak	IIIA	1,426	19,580	2.925	1.0393
Casas Grandes	IIIA	381.8	3,732	4.114	1.1296
Charcas	IIIA	149.3	1,117	5.386	1.2301

stant of 1.59 ± 0.050 × 10^{-11} year^{-1} was later measured experimentally by Lindner and co-workers (*16*) and subsequently refined by Lindner and co-workers to be 1.639 ± 0.050 × 10^{-11} year^{-1} (*17*). If the latter decay constant is used with the isochron of Luck and Allègre (*14*), an age of ~4200 Ma is indicated for combined iron groups, suggesting that crystallization occurred ~300 million to 400 million years after the initiation of the formation of the solar system (*15, 17*). However, Morgan and co-workers (*18*) report a steeper isochron slope for pooled IIAB and IIIAB iron meteorite data (0.0792 ± 0.0020) than was obtained by either Luck and Allègre (*14*) or Walker and Morgan (*15*). The analytical differences between the results of Morgan and co-workers (*18*) and those of Walker and Morgan (*15*) were the result of a recalibration of the Re spike that showed it was 6% less concentrated than previously thought (*19*). In this study, we investigate the chronology of iron meteorites further using higher precision negative thermal ionization techniques than were used by Morgan and co-workers (*18*). The high precision provides the resolution necessary to detect isotopic differences between the iron groups.

Separation procedures for Re and Os have been detailed (*20–22*). Total analytical blanks, including loading and filament blanks, were approximately 100 pg for Re and 90 pg for Os (*23*). Mass spectrometric procedures were similar to those described by Creaser and co-workers (*24*). Osmium was measured as OsO_3^- and Re as ReO_4^- (*25*) (Table 1). Duplicate analyses of Coahuila (Table 1) show that the Re and Os concentrations and the Os isotopic compositions agree to within ±1 per mil of the average. As a consequence of the agreement of analyses made by two different mass spectrometers and the duplicate analysis of Coahuila, we estimate 2σ precisions for ^{187}Os/^{186}Os and ^{187}Re/^{186}Os ratios of 1 per mil and 3 per mil, respectively. Because of the larger proportion of Re blank for Mount Joy, a 2σ precision for its ^{187}Re/^{186}Os ratio of 5 per mil is estimated.

All data for IIA iron meteorites plot within the uncertainty of an isochron that defines a slope of 0.07824 ± 0.00053 and an intercept of 0.8007 ± 0.0029 [model 3 fit, 2σ from scatter (*26*)] (Fig. 1). The uncertainty in the slope is equivalent to ±31 million years for meteorites that are ~4500 million years old. The intercept is in good agreement with the previously published values for irons (*13, 14, 18*) and is also similar to the initial ratio of 0.802 ± 0.049 determined for carbonaceous chondrites (*15*). The absolute closure age for the IIA iron group is 4596 ± 152 million years, with the total uncertainty resulting from uncertainties in the decay constant reported by Lindner and co-workers (*17*) (3%), the slope of the isochron (0.6%), and the calibrations of the Re and Os spikes (total of 1%). The age of all iron meteorites, however, is probably less than the maximum age of 4560 Ma for chondrites (*11*), because irons are much more chemically evolved than chondrites. Therefore, the results suggest that the IIA irons crystallized between 4560 and 4444 Ma.

Data for the IA iron Canyon Diablo, IIB iron Mount Joy, and three group IIIA irons, Costilla Peak, Casas Grandes, and Charcas, all plot significantly above the IIA isochron (Fig. 1). These data can be interpreted in at least four ways. First, some of these irons could conceivably be plotting on separate isochrons with steeper slopes than the isochron generated by the data for the IIA irons. Thus, they might record older Re-Os closure ages than for the IIA irons. This is unlikely for most of these meteorites, especially Costilla Peak, because the slope of any such isochron with an initial ^{187}Os/^{186}Os ratio of approximately 0.800 would give unreasonably old ages, even when the uncertainty in the ^{187}Re decay constant is factored in. For example, for an intercept of 0.800, the youngest age of Costilla Peak could be 4730 Ma for a decay constant of 1.66 × 10^{-11} year^{-1}.

A second interpretation is that all the irons became closed systems to Re and Os movement at approximately the same time, but that the parent bodies of the different iron groups either formed with different Os isotopic compositions or evolved to different Os isotopic compositions before core formation. Such differences could have resulted if there were different Re/Os ratios in the parent bodies or their precursor materials and sufficient time. For example, if the parent bodies of the IIAB and IIIAB irons formed within 20 million years of the earliest formation of chondrite components, the precursor materials must have had ^{187}Re/^{186}Os ratios >10 in order to achieve the maximum 1% isotopic heterogeneity observed. Such high Re/Os ratios are unlikely to have been present on a large (asteroidal) scale because iron meteorites likely differentiated from small planetary bodies that ac-

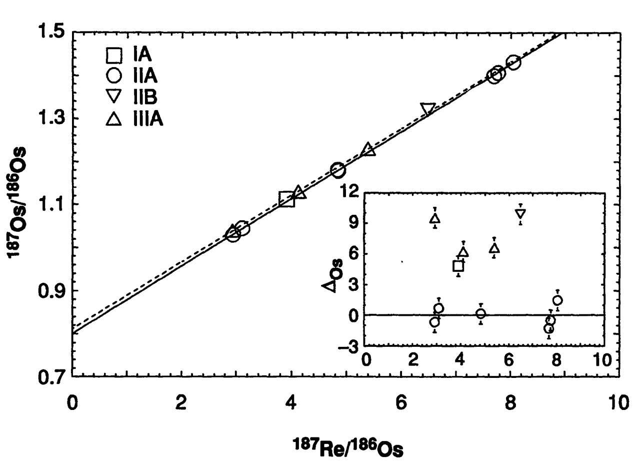

Fig. 1. Plot of ^{187}Os/^{186}Os versus ^{187}Re/^{186}Os for iron meteorites. Note that the symbols are much larger than the uncertainty. Isochrons are regressed through IIA data (solid line) and IIIA data (dashed line). The slope of the IIA isochron is 0.07824 ± 0.00053 with an intercept of 0.8007 ± 0.0029. The slope of the IIIA isochron is 0.0775 ± 0.0018 with an intercept of 0.8120 ± 0.0075. The inset shows Δ_{Os}, the per mil deviation in ^{187}Os/^{186}Os from the IIA isochron, versus ^{187}Re/^{186}Os. Uncertainty in the ^{187}Os/^{186}Os ratio is shown to the correct scale (±1 per mil), although the effects of uncertainty in the Re/Os ratio are not shown.

creted with chondritic Re/Os ratios. The ^{187}Re/^{186}Os ratios of enstatite and carbonaceous chondrites are 4 or less (*15, 27*).

A third interpretation is that Os isotopic heterogeneities may have existed in the solar nebula. Thus, Os could have been heterogeneous like O, which apparently had different isotopic compositions in different parent bodies (*28*). The data of Luck and Allègre (*14*) and Walker and Morgan (*15*) indicate that some types of chondrites may have initial Os isotopic ratios different from those of most iron groups. Hence, it is possible that the apparent heterogeneities observed in the iron meteorites could result from a similar, though as yet undefined process.

A final interpretation is that irons with Re-Os systematics that plot above the IIA isochron became closed to Re and Os movement after the IIA irons did. For example, the data for the three IIIA irons can be regressed to give an isochron with a slope of 0.0775 ± 0.0018 and an intercept of 0.8120 ± 0.0075. This slope is within the uncertainty of the slope obtained for IIA irons, although there is no overlap in the uncertainties for initial ratios. An age of 4554 ± 105 Ma, compared with 4596 ± 31 Ma for the IIA irons, is calculated with the decay constant of 1.639×10^{-11} year^{-1}, assuming errors only for the regressions. A maximum age differential of 178 Ma is thus possible between the IIA and IIIA irons within the stated uncertainties. In consideration of this maximum age differential, a first-stage ^{187}Re/^{186}Os ratio of 3.9 would have been necessary to change the initial ^{187}Os/^{186}Os ratio from 0.8007 for the IIA irons to 0.8120 for the IIIA irons. Such evolution is plausible in that the average ^{187}Re/^{186}Os ratio for these three samples is 4.14, similar to the ratios for chondrites. One problem with this simple two-stage model is that the presence of excess ^{107}Ag (a decay product of the short-lived isotope ^{107}Pd) in IIIA Cape York and IIIB Grant (*9, 10*) indicates that ^{107}Pd was incorporated into the IIIAB parent body core and variably partitioned as a result of magmatic fractionation. This may limit the maximum possible age of core formation to within approximately 65 million years of nucleosynthesis. Closure age differences between the IIAB and IIIAB groups of less than 65 million years are permitted by the Re-Os data if the precursor material to the IIIAB irons had a ^{187}Re/^{186}Os ratio greater than 10. However, as discussed above, such large ratios are well above the range for chondrites.

As with the IIIA irons, the isotopic compositions of both the IA Canyon Diablo iron and the IIB Mount Joy iron might also be consistent with Re-Os system closure after closure in the IIA irons. Mount Joy probably crystallized as a result of the same magmatic fractionation processes (and from the same parent body) that produced the IIA irons. However, the IIB irons are more fractionated and, consequently, were likely derived from a melt system with a relatively high ^{187}Re/^{186}Os ratio. The melt from which they precipitated probably had a higher Re/Os ratio than that of the most highly fractionated IIA irons, such as Lombard (^{187}Re/^{186}Os = 8.042). Thus, the systematics of Mount Joy, which plots about 10 per mil above the IIA isochron, may be indicative of a closure age that is on the order of 40 to 50 million years younger than the IIA closure age. This time interval cannot be significantly longer because excess ^{107}Ag is present in the IIB iron DRPA78009.8 (*10*).

Any of the first three interpretations of the Os isotopic data have significance. If the parent body cores were isotopically heterogeneous as a result of the variable rates of ^{187}Os growth in the differentiating parent bodies, the parent bodies could not have been chondritic with respect to their Re/Os ratios. No samples of such unusual material have yet been identified. If the iron parent bodies were initially heterogeneous with respect to Os upon accretion, then there may have been some relation between the Os isotopic composition and the location of the parent body, such as has been discussed regarding O isotopic heterogeneities (*28*). This could ultimately prove to be a useful tool in identifying meteorite source regions. If the closure ages of the various iron groups are different, it seems likely that the sizes, hence cooling rates, of the parent bodies must have varied considerably. This notion leads to the interpretation that the IIAB irons were derived from a relatively small parent body that could cool rapidly compared with the IIIAB parent body.

In summary, the data indicate that the Re-Os isotopic systematics of iron meteorites are variable, although consistent within groups. The group IIA iron meteorites have Os isotopic systematics that became closed near the canonical age of the solar system. Their initial ^{187}Os/^{186}Os ratio was the same as that of carbonaceous chondrites to within reported uncertainties. The data for the three IIIA irons may indicate either a later closure age, and a correspondingly higher initial ^{187}Os/^{186}Os ratio, or heterogeneous initial compositions. The Re-Os system permits the two groups to have closed as much as 178 million years apart, although the presence of excess ^{107}Ag in IIIAB irons argues against such a large disparity. But a lower age difference would require a much higher ^{187}Re/^{186}Os ratio than has been observed in chondrites in the precursor material to the IIIA parent body. The closure ages for the IA Canyon Diablo iron and the IIB Mount Joy iron may also be younger than that of the IIA irons.

The observation that the IIA and IIIA iron meteorites plot on different isochrons indicates that the Re-Os system can be used as a chronologic tool to determine the absolute ages of different iron groups. It is likely that separated phases may provide greater ranges in Re/Os ratios so that higher precision dating (better than 0.5%) can be achieved in the future. The chief limitation to absolute dating of irons with this system is the uncertainty in the decay constant for ^{187}Re. It is likely that this problem will be rectified by the study of terrestrial systems with independently determined ages.

REFERENCES AND NOTES

1. E. Pernicka and J. T. Wasson, *Geochim. Cosmochim. Acta* **51**, 1717 (1987).
2. S. Niemeyer, *ibid.* **44**, 33 (1980).
3. D. S. Burnett and G. J. Wasserburg, *Earth Planet. Sci. Lett.* **2**, 397 (1967).
4. H. G. Sanz, D. S. Burnett, G. J. Wasserburg, *Geochim. Cosmochim. Acta* **34**, 1227 (1970).
5. D. S. Burnett and G. J. Wasserburg, *Earth Planet. Sci. Lett.* **2**, 137 (1967).
6. N. H. Evenson *et al.*, *Lunar Planet. Sci.* **X**, 376 (1979).
7. W. R. Kelly and G. J. Wasserburg, *Geophys. Res. Lett.* **5**, 1078 (1978).
8. T. Kaiser and G. J. Wasserburg, *Geochim. Cosmochim. Acta* **47**, 43 (1983).
9. J. H. Chen and G. J. Wasserburg, *ibid.*, p. 1725.
10. ———, *ibid.* **54**, 1729 (1990).
11. ———, *Earth Planet. Sci. Lett.* **52**, 1 (1981).
12. W. Herr *et al.*, *Z. Naturforsch. Teil A* **16**, 1053 (1961).
13. J. M. Luck *et al.*, *Nature* **283**, 256 (1980).
14. J. M. Luck and C. J. Allègre, *ibid.* **302**, 130 (1983).
15. R. J. Walker and J. W. Morgan, *Science* **243**, 519 (1989).
16. M. Lindner *et al.*, *Nature* **320**, 246 (1986).
17. M. Lindner *et al.*, *Geochim. Cosmochim. Acta* **53**, 1597 (1989).
18. J. W. Morgan, R. J. Walker, J. N. Grossman, *Earth Planet. Sci. Lett.*, in press.
19. We conducted the Re and Os spike recalibrations in June 1991, using negative thermal ionization mass spectrometry. The recalibrations indicated that the Re concentrations reported by Walker and Morgan (*15*) were 6% too high, but that Os concentrations were not significantly different. Another set of Re calibrations was analyzed to confirm this finding, and it provided similar results. The concentrations of Re and Os in the spikes used in both (*18*) and this study are now likely accurate to within 0.5% of their true concentrations. The reason for the initial inaccuracy in spike calibration has not been determined but could have resulted from a weighing error or unsatisfactory spike-standard equilibration.
20. J. W. Morgan and R. J. Walker, *Anal. Chim. Acta* **222**, 291 (1989).
21. J. W. Morgan *et al.*, *Talanta* **38**, 259 (1991).
22. Rhenium and Os concentrations were determined by isotope dilution. Samples were spiked with ^{190}Os and ^{185}Re enriched isotopes and dissolved in HCl; the dried residue was then fused with a sodium hydroxide–sodium peroxide mixture.
23. The blanks resulted primarily from the Re and Os contained in the zirconium crucibles in which irons were fused. The blanks comprised <0.1% of the total Re and Os in all samples except Mount Joy for which the Re blank constituted about 0.8%. Hence, they had no significant effect on these measurements except for the larger Re uncertainty of Mount Joy.
24. R. A. Creaser, D. A. Papanastassiou, G. J. Wasser-

burg, *Geochim. Cosmochim. Acta* **55**, 397 (1991).

25. Rhenium and Os isotopic data were corrected for ^{17}O and ^{18}O species, and Os data were corrected for spike contributions to minor isotopes. We also corrected isotopic data for fractionation, using a ^{192}Os/^{188}Os ratio of 3.08271 (*14*). Under all run conditions fractionation was <1 per mil per atomic mass unit. In the isotopic analyses we used two thermal ionization mass spectrometers: a 12-inch radius of curvature, 90° sector machine at the National Institute of Standards and Technology, Gaithersburg, MD, and the 12-inch radius of curvature, 68° sector, Bobcat 1 instrument at the University of Maryland, College Park. All measurements were made with single faraday cup detectors. Signals of >1 V and >10 mV were obtained for major and minor isotopes, respectively. Each Os isotopic composition was measured on both mass spectrometers as a check on the external precision of the mass spectrometry. Each isotope ratio was measured to a 2σ (mean) precision better than 1 per mil; the ratios obtained by each mass spectrometer agreed to within ±1 per mil of the average. We determined the ^{187}Os/^{186}Os ratio of each sample both directly and by measuring the ^{187}Os/^{188}Os ratio and converting to a ^{187}Os/^{186}Os ratio using a ^{186}Os/^{188}Os ratio of 0.11990. The measured and the calculated ratios agreed to within ±1 per mil.
26. K. Ludwig, *U.S. Geol. Surv. Open File Rep. OF 88-0557* (1988).
27. J. W. Morgan, R. J. Walker, J. N. Grossman, *Lunar Planet. Sci.* **XXI**, 809 (1990).
28. R. N. Clayton, T. K. Mayeda, E. J. Olsen, M. Prinz, *Earth Planet. Sci. Lett.* **65**, 229 (1983).
29. We thank R. S. Clarke of the Smithsonian Institution for meteorite samples, the Mass Spectrometry Group of the National Institute of Standards and Technology for the use of various mass spectrometers and for donating portions of Bobcat 1, and W. A. Bowman for helping with the Bobcat 1 instrument. Discussions with S. B. Shirey were helpful. Early drafts of this manuscript benefited from the reviews of R. Brett, P. Baedecker, J. Wasson, and an unidentified reviewer. This research was partially supported by National Aeronautics and Space Administration contract 91-143.

17 October 1991; accepted 2 January 1992

Overlapping Nucleotide Determinants for Specific Aminoacylation of RNA Microhelices

CHRISTOPHER FRANCKLYN,* JIAN-PING SHI, PAUL SCHIMMEL

A seven–base pair microhelix that recapitulates a glycine transfer RNA (tRNA) acceptor helix can be specifically aminoacylated with glycine. A single base pair and the single-stranded discriminator base near the attachment site are essential for aminoacylation. These nucleotide sequence elements, and those in microhelices that can be charged with histidine and alanine, occur in the same positions and therefore overlap. Studies on a systematic set of sequence variants showed that no microhelix could be charged with more than one amino acid. Also, none of the three cognate aminoacyl-tRNA synthetases (aaRSs) gave a detectable amount of aminoacylation of the CCA trinucleotide that is common to the 3′ ends of all tRNAs, showing that the specific acceptor stem nucleotide bases confer aminoacylation. An analysis of the relative contributions of these microhelices to overall tRNA recognition indicates that their interaction with aaRSs constitutes a substantial part of the recognition of the whole tRNAs.

THE AMINO ACID ACCEPTOR STEM and the anticodon are common locations of the major determinants of aminoacylation specificity (*1, 2*). The acceptor stem is itself a substrate for alanine and histidine aaRS (*3–6*). In these cases, each respective tRNA has been shown to have its major determinant located in the acceptor stem [G3:U70 for tRNA^{Ala} (*2, 3*) and the unique G−1:C73 for tRNA^{His} (*6, 7*)]. These observations, the early proposal (*8*) [substantiated by recent experiments (*4, 9–12*)] that the N73 nucleotide in the acceptor stem acts in general as an important part of the system of tRNA identity elements, and the highly differentiated interactions between acceptor helix elements and synthetases that have been elucidated in the three-dimensional structures of *Escherichia coli* tRNA^{Gln} (*13, 14*) and *Saccharomyces cerevisiae* tRNA^{Asp} (*15*) with their respective enzymes suggest that further examples of amino acid–specific aminoacylation of acceptor stem microhelices might be found. As an additional possibility, we investigated a tRNA for which anticodon nucleotides are implicated as at least part of the tRNA identity system. Early genetic studies suggested that Gly tRNA synthetase recognizes the anticodon nucleotides C35 and C36 (*16*). However, alteration of the tRNA$^{Gly}_{CCC}$ anticodon to CUA yields an efficient Gly-inserting amber suppressor (*17*), suggesting that, for this isoacceptor, nucleotide determinants outside of the anticodon are also important for aminoacylation. The conservation of the first four acceptor stem base pairs and U73 among all three tRNA^{Gly} isoacceptors (*18*) prompted us to design a set of oligonucleotide substrates with potential Gly acceptor stem determinants, both alone and in conjunction with determinants for Ala and His.

We found that a seven–base pair microhelix based on the acceptor stem sequence of tRNA$^{Gly}_{CCC}$ can be specifically aminoacylated with Gly (micro^{Gly}, Fig. 1A). The charging by GlyRS was less than the rate of aminoacylation of micro^{Ala} and micro^{His} with their cognate enzymes (*19*). The kinetic parameters for micro^{Gly} aminoacylation with purified GlyRS were as follows: the Michaelis constant $K_m = 45\ \mu\text{M}$ and the rate constant $k_{cat} = 3 \times 10^{-3}\ \text{s}^{-1}$; for aminoacylation of tRNA^{Gly} under similar conditions, $K_m = 0.6\ \mu\text{M}$ and $k_{cat} = 3.5\ \text{s}^{-1}$. Neither micro^{Ala} nor micro^{His} was aminoacylated with Gly, which suggests that although the charging of micro^{Gly} by GlyRS was less efficient than the charging of microhelices by the other two aaRSs, aminoacylation of microhelices by GlyRS is sequence specific.

Because micro^{Gly} retained specificity for Gly and could not be misacylated with other amino acids, we predicted that, as in the case of micro^{Ala} and micro^{His}, aminoacylation of Gly microhelices might also be dependent on one or more sequence determinants among the nucleotides found at N73, 2:71, and 3:70. To characterize the effect of these potential determinants on each of the three aaRSs, we constructed 13 sequence variants based on a reference stem-loop sequence (Fig. 1B). In the 13 variants selected, sequences from the cognate microhelices (Fig. 2, constructs 1, 6, and 13) were grouped in different combinations to help to identify sequences necessary for Gly acceptance. Constructs 1, 6, and 13 contain the nucleotides at positions N73, 2:71, and 3:70 that are unique to the isoacceptors of tRNA^{Ala}, tRNA^{His}, and tRNA^{Gly}, respectively, in the context of the reference stem-loop.

As observed with the parental microhelix (Fig. 1A), there was no aminoacylation of microhelices 1, 6, and 13 with either of the other two noncognate amino acids (Fig. 3). These variants were aminoacylated by their cognate enzymes with efficiencies equal to those of their parental variants. Thus, the specificity and efficiency of aminoacylation is retained in the context of the reference structures and is largely determined by the 2:71, 3:70, and N73 nucleotides.

The 13 sequence variants were tested individually as substrates for aminoacylation by each of the three aaRSs. Each aaRS aminoacylated a unique subset of these 13 variants, and none of the variants was aminoacylated by more than one enzyme (Fig. 2). Sequence determinants in microhelices specific for GlyRS were studied with all of the constructs. The most efficient aminoacylation was achieved with the G3:C70,

---

Department of Biology, Massachusetts Institute of Technology, Cambridge, MA 02139.

*Present address: Department of Biochemistry, University of Vermont College of Medicine, Burlington, VT 05405.